Digital Image Correlation for Non-Homogeneous Biomaterials

A Thesis presented by:

Fereshteh Safavinia

Supervised by:

Dr. Morshed Khandaker

Presented to the Jackson College of Graduate Studies of the University of Central Oklahoma in Partial Fulfillment of the requirements for the Degree of

Master of Science in Electrical Engineering
University of Central Oklahoma
Edmond, Oklahoma
May, 2019

Digital Image Correlation for Non-homogeneous Biomaterials

Thesis Approved:

Committee Chair: Dr. Morshed Khandaker

Committee Member: Dr. Alaeddin Abuabed

Committee Member: Dr. Yuhao Jiang

Committee Member: Dr. Susmita Hazra

Acknowledgements

I feel much honored to say that due to keen knowledge of the faculties it was very easy for me learn extensive knowledge regarding “Digital Image Correlation for Non-homogenous biomaterials.”

I have taken efforts in this research; however, it would not have been imaginable without kind support and guidance of many individuals.

I would like to appreciate to the Department of Engineering and Physics, the College of Mathematics and Science, and Graduate collage at University of Central Oklahoma.

I would like to thank Professor Morshed Khandaker for his support and his contribution of ideas and his encouragement.

I also like to thank Dr. Alaeddin Abuabed, Dr. Yuhao Jiang, and Dr. Susmita Hazra who provided insight and expertise that greatly assisted the research.

Secondly, I also like to thank my husband for his continuous support throughout this academic journey.

Abstract

The Digital Image Correlation (DIC) is the optical and noncontact method to measure deformation and full-field strain of a loaded object. In general, DIC method is used for homogenous materials, whose composition, shape, and texture are the same throughout the materials like aluminum and copper. There is no established DIC method for a non-homogenous material, which is not uniform, such as bi-material interface surfaces. The goal of this study is to apply DIC method to a non-homogeneous system to evaluate the mechanical response due to applied load. In this study, DIC method was applied to three different non-homogeneous systems: metal/cement, bone/cement and multi-layers' fiber cloth.

The first objective was to measure the strain at the interface of aluminum and cement by using DIC method. In order to understand the deformation characteristics, a series of images were taken by high speed camera, Phantom V641. Using a Matlab program of DIC method, the full-strain at the interface was found. The second objective was to find the full strain at the interface of bone-cement-aluminum in a knee replacement surgery. The third objective was to find the strain of the rolled fiber cloth that can be used for biomedical applications. The fiber was obtained from the existing electrospinning system and the procedure was repeated to find the strain value of the fiber.

The research successfully measured the deformation characteristics of aluminum – cement interface using DIC method and compared the values with mechanical of materials theoretical values. This study also measured deformation characteristics of bone-cement- aluminum interfaces for a total knee replacement system and compared the values with the computer model. Finally, the strain field of rolled fiber was measured and compared the values with a plastic material model. The DIC protocol developed in this study can be used to measure the properties of the materials around the interface of two bi-materials and multi-layers' fibrous materials. The developed techniques will be useful for the development and design of orthopedic biomaterials.

TABLE OF CONTENTS

LIST OF FIGURES

LIST OF TABLES

LIST OF ABBREVIATIONS

DIC……. Digital Image Correlation

Pixel…… A picture element

Grayscale……..... The range of brightness in digital image

Subset……. An area of some pixels

NCC……... Normalized Cross Correlation

ZNSSD…..……Zero Normalized Squared Sum of Differences

CHAPTER 1

DIGITAL IMAGE CORRELATION

1.1 Introduction

Digital image correlation, DIC, is a noncontact and optical method to measure deformation characteristic of a system that can be applied in most sciences and engineering. DIC method is applied for deformation measurements of the materials in the range of micro-meter per meter. DIC method uses image processing technique for deformed objects. This method is based on the light intensity patterns in a series of digital images taken during the object deformations. Strain gauge, extensometers, or optical interferometry can be used to measure displacement and strain fields for homogeneous materials, whereas, the DIC method can be used for non-homogeneous material deformation. However, there are some advantages of using DIC method to conventional methods such as a noncontact method, ability to apply for a huge range of applications, more accurate results, and it is not necessary to time consuming set up. Many researches have showed the potential of DIC method in the measurements of experimental mechanics. Digital image correlation is the main focus of this study to solve a problem in the strain field, particularly for the non-homogenous materials.

1.2 Digital Image Correlation

1.2.1 Background

Digital image correlation has been introduced for over thirty years. Gilbert Hobrough (1919-2002) performed some of the first work in this method “and built an instrument to correlate high-resolution reconnaissance photography with high precision survey photography in order to enable more precise measurement of changeable ground conditions” [1]. Improving

digital computers led to processing and obtaining information from digital images [2] that first analyzed images such as text, photomicrographs, and nuclear particle tracks. Also, researchers started to use vision-based algorithms and applications of photogrammetry for aerial photographs [3]. Many algorithms and models were written to analyze images between 1950-1960 that were expanded to get the three-dimensional information of sequence images taken by an analog camera. Documents of advances in this method between 1955-1979 are found in the paper [2]. Digital image processing first focused on the fields such as character recognition, microscopy, medicine and radiology. Then, parallel to developing of laser technology, it was applied for laser speckle, laser speckle interferometry [4], holographic interferometry, and so forth. The difficulties of processing the recorded data photographically in mechanical experiment led the researchers to develop methods for taking digital images, writing new algorithms to extract the accurate measurement data.

1.2.2 History

The mechanical engineering department of the University of South Carolina developed the DIC technology, digital image correlation, in the mid-1980s [5].Then, digital image correlation was developed in the correlation algorithms, the time of procedure, and the accuracy of correlation. The next section will review in the improvement of correlation algorithms.

For the first time in 1980[6], Peters and Ranson from Department of Mechanical Engineering in the University of South Carolina introduced a new method, DIC, to measure the displacement of a surface by employing an algorithm of cross-correlation for a subset of pixels to correlate them throughout the images before and after deformation.

An improvement of the new method was written by Sutton *et al*. in 1983 [7]. They placed a cantilever beam covered by random speckle normal to the axis of a camera. A series of images were taken before and after deformation. A set of grey levels indicated the intensity of light for each image. Then, the correlation coefficient was used to find the displacement parameters. More explanation and assumptions in DIC method were explained by Chu *et al*. [8] that were accurate in deformation of rigid body. In 1986 and 1989, the Newton-Raphson method [9] was applied to improve DIC algorithm. Hovis suggested a suitable method for small deformation in the two-dimensional displacement measurement problem [10]. In this method, the initial displacements were not necessary because the centroids of speckles were tracked in subsequent images. The Geometric Approach equation was used to find the strain components. Fast-Fourier Transform, FFT, was used to find the full-field displacement by Chen in1993. In this way, first, some subsets in reference and deformed images were selected to find their complex spectra and the resultant spectra using the phase difference of complex spectra. Second, the FFT would find the considerable signal peak then the displacements, u and v, were determined. This method was not successful for large deformation and rotation. During 1993 to 2009, further optimized in Newton-Raphson (NR) and peak-finding algorithm method were introduced, but these improvements still were neither accurate nor fast. In 2009, Pan used Zero-Normalized Cross-Correlation (ZNCC) to find the deformation in two dimensions. He selected an area with 5 or 10 points in the first image and found the ZNCC maximum correlation between these points in first image and the corresponding points in the deformed image to find the ZNCC coefficient. In 2011, Pan and Li [11] proposed a fast DIC method to measure deformation. This work was based on the NR-algorithm with eliminating the repeating calculation in integer-displacement searching [12]. Also, a pre-computed global interpolation coefficient table was used to avoid repeating

calculating in interpolation for the position of subpixels. Zhou and Chen [13] employed a propagation function in 2012 to get a better estimation of initial parameters of deformation. Their results were more accurate especially when the deformation is in the subset area and eliminated some iterations to get the optimization to converge. In this work, the parameters of deformation for adjacent points are related by the propagation function. In 2012, Pan *et al.* addressed an incredible method [14], Incremental DIC, to overcome decorrelation in large deformation and in illumination variations. In incremental DIC, first, images 1 and 2 are correlated to find the deformed position of original grid. Second, the adapted grid is created around deformed positions. Third, image 2 (with adapted grid) and image 3 were correlated to find the deformed position of adapted grid in image 3. To find the total deformation between image 1 and 3, the results of adapted grid are added to the results of image 1 and 2. This process is repeated for all subsequent images. Jiang *et al.* [15] introduced a new technique to speed up the computation of Hessian matrix using the integral image in 2015. In integral image, the sum of the values of subset of a grid is calculated quickly. Recently, other researchers have proposed different algorithms to reduce the time of computation and to get the more accurate results in DIC method.

1.2.3 Execution process

I. Digital image processing

A digital image is divided by many elements: pixels, arranged in a matrix with the known number of rows and columns [16]. A pixel is represented by the number of bits showed the intensity of that pixel. In digital image, 8-bit positive integer corresponds to intensity of each pixel in a range of 0 to 2^8 (256) to present different shades, grayscale. Values of 0 presents black, and 256 white, high intensity. Each value between 0 and 256 displays a shade of gray. Figure 1.1

is an example of grayscale values of a digital image.

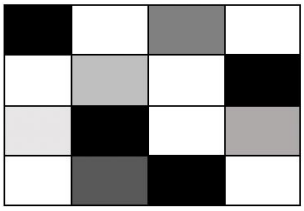

$$\begin{bmatrix} 0 & 256 & 170 & 256 \\ 0 & 100 & 256 & 0 \\ 60 & 0 & 256 & 150 \\ 256 & 200 & 0 & 256 \end{bmatrix}$$

Figure 1.1: A digital image and corresponding intensity

Resolution of an image presents the number of pixels in that image for example 2560 ×1600 resolution presents about 4×10^6 pixels in an image.

Since a pixel value repeats many times in an image, it is not possible to track a pixel in the image processing. For this reason, an area of some pixels, subset, is determined to process which has a specific brightness distribution.

II. Correlating of images

In the digital image correlation, a subset in the image before deformation will track in the image after deformation to find the same brightness distribution in the first image. Different complex algorithms, talked about in the section 1.2.2, were written for this process. Figure 1.2 shows two images before and after deformation in the left and right side, respectively. The square in the left image presents the selected subset with a unique intensity, and the square in the right image has the same intensity. Thus, the subset in the right image is the new position of the subset in the left image after applying deformation.

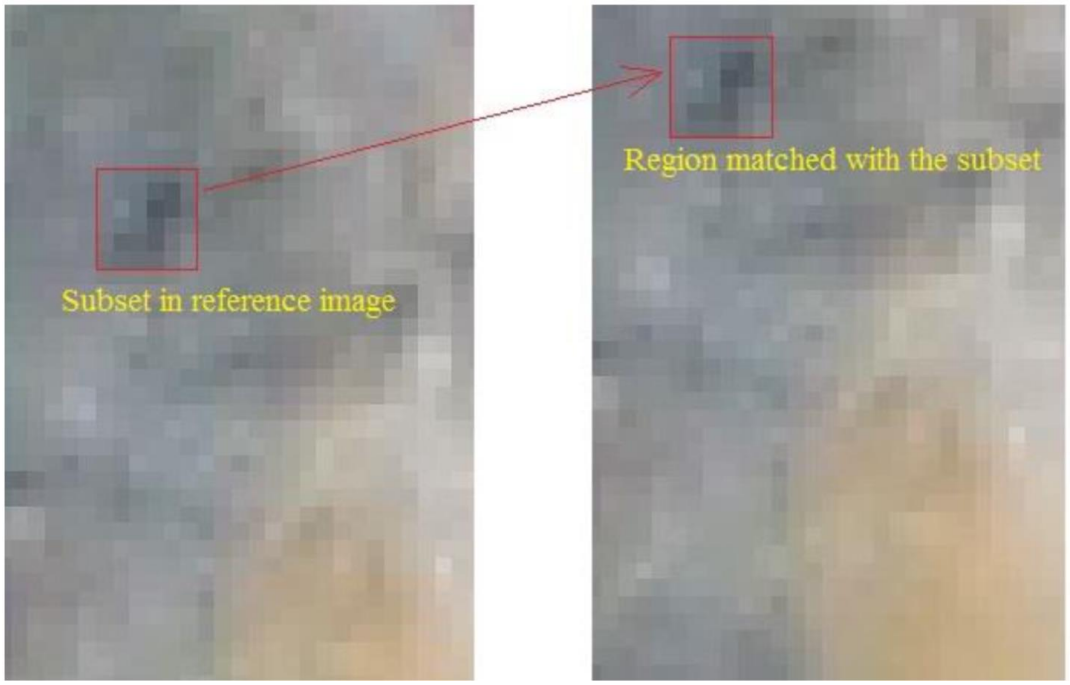

Figure 1.2: The two subsets in the images before (left) and after (right) deformation with the same brightness. Retrieved from [17].

Therefore, the displacement of the center of this subset can be calculated. The selected subset should have n × n pixels where n is large enough and an odd number. In the section Speckle pattern, the size of subset will be discussed. Also, the center of subset is defined as a single pixel with an odd number of n.

III. Speckle pattern

Speckle pattern is applied on the surface of the specimen to compensate one of the problems in image matching that is aperture problem [3] as shown in Figure 1.3[3].

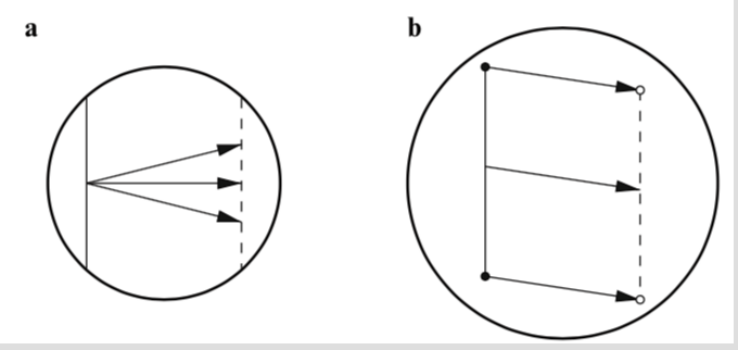

Figure 1.3: The aperture problem in the image matching. a) A point can match with some points on the displaced line. b) Enlarged aperture. Retrieved from[3]

Since a single pixel in the first image can match with thousands of other pixels in the second picture, a region around a pixel should be chosen in the first image to find the correspondence of that pixel in the second images. The neighborhood should be large enough. In the figure 1.3 (a), a line in the image is selected. The component of motion that is orthogonal to the line can be resolved while the component along the line cannot. By increasing the aperture, in Figure 1.3 (b), the end points of the line are located in aperture and the vector of motion can be determined. This problem is more difficult to solve where an object without texture tolerates deformation because any characteristic is not inside the aperture. A non-periodic surface texture is recommended to solve a correspondence problem in translation or deformation of specimen. Speckle pattern is the best choice of a random pattern as shown in figure 1.4 [18].

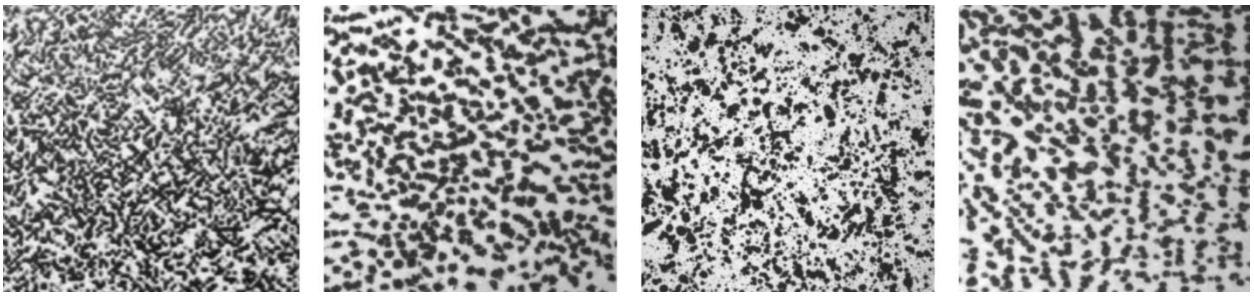

Figure 1.4: The speckle pattern on the surface of sample. Retrieved from[18]

This random pattern is adhered on the entire surface of the specimen, so small aperture can be chosen to find correspondence between two images due to the translations or deformations.

IV. Correlation coefficient evolution

The Correlation Coefficient is the suitable measure to find the similarities between two functions that is a number between -1 and 1[19]. If the two function are g(t) and z(t) advanced by τ, the Cross Correlation is defined by equation (1.1):

$$\psi(\tau) = \int_{-\infty}^{\infty} Z(t)g(t-\tau)dt \qquad (1.1)$$

In the paper[20], the normalized form of cross correlation was introduce to solve some issues to find correlation coefficient(refer to the paper).

In this algorithm, the squared Euclidean distance was used as equation (1.2):

$$d^2_{f,\,t}\,(u, v) = \sum_{x,y} [f(x,y) - g(x-u, y-v)]^2 \qquad (1.2)$$

where f and g are the functions of light intensity at (x, y) and at (x-u, y-v), respectively and Σ is the sum of the values within the subset.

The expansion of (1.2) is:

$$d^2_{f,t}(u, v) = \sum[f^2(x, y) + g^2(x-u, y-v) - 2 f(x, y)\, g(x-u, y-v)] \quad (1.3)$$

The term [Σ f (x, y) g (x-u, y-v)] is the cross correlation and can be used to find the similarity between the two interested regions since term $\sum g^2(x-u, y-v)$ is constant and $\sum f^2(x, y)$ is approximately constant.

Although in transform domain, the cross correlation term can be used adequately, there are some problems using this term alone, such as[21]:

- It is not easy to interpret the scoring value.
- If the two functions have the same shape with different amplitude, the correlation is not equal 1.
- since the result of any number times zero is equal zero, the account does not detect the zero value.

To overcome these difficulties, the Normalized Cross Correlation, equation (1.4), was proposed:

$$\gamma = \frac{\Sigma[f(x,y)-f_m][g(x-u,y-v)-g_m]}{\{\sum_{x,y}[f(x,y)-f_m]^2 \sum_{x,y} g(x-u,y-v)-g_m]^2\}^{0.5}} \quad (1.4)$$

where f_m and g_m are the mean of functions f and g, respectively.

Although the Normalized Cross Correlation is used in this paper, it is productive to explain the Zero- Normalized Sum of Squared Difference for future work.

Since the intensity of the deformed subset is different from the original subset, the similarity will be reduced. As a result, correlation criterion can be considered by zero-mean normalized sum of squared difference[22]. If f (x, y) is the distribution of reference subset at x-y coordinates, f_m, the average distribution values in that subset, is calculated by equation (1.5):

$$f_m = \frac{1}{(2M+1)\,\hat{}\,2} \sum_{x=-M}^{M} \sum_{y=-M}^{M} | f(x,y) | \quad (1.5)$$

Where M is the range of subset.

Similarity, g (x^*, y^*) and g_m are distribution value of deformed subset and average of the deformed subset, respectively. In Eq. (1.6), g_m is defined.

$$g_m = \frac{1}{(2M+1)\,\hat{}\,2} \sum_{x=-M}^{M} \sum_{y=-M}^{M} | g(x*, y*) | \quad (1.6)$$

The Zero- normalized sum of squared difference is given as Eq. (1.7) [23]:

$$C_{ZNSSD} = \sum_{x=-M}^{M} \sum_{y=-M}^{M} \left[\frac{f(x,y) - f_m}{\sqrt{\sum_{x=-M}^{M} \sum_{y=-M}^{M} | f(x,y) - f_m |\,\hat{}\,2}} \right. \quad (1.7)$$

$$\left. - \frac{g(x*,y*) - g_m}{\sqrt{\sum_{x=-M}^{M} \sum_{y=-M}^{M} | g(x*,y*) - g_m |\,\hat{}\,2}} \right]^2$$

and summations are over the points in subset areas.

1.3 Homogeneous materials

A material, whose composition and properties are uniform throughout it , is called homogenous[24] for examples metals, alloys, ceramics, polypropylene, steel, glass, and nylon. The term of homogenous is used in the fields like physics, chemistry, and nature. In mixture materials, the components that are mixed in a homogenous material cannot be identified separately. If a property of homogenous material along X is f (x), f (x) should be constant that means the properties of these materials do not depend on the orientation.

1.4 Non-homogeneous materials

In physics, a material is non-homogenous whose physical properties vary through its medium for example powder-coated steel, plywood, and laminate. A mixture of non-homogenous consists of different phases and substances[25]. In this study, the producing of one example of non-homogenous material, multi-layers' fiber, is presented to show the difference of its physical properties throughout its length.

1.5 Problems of DIC method for non-homogeneous materials

Although DIC method has the powerful potential to find the deformation characteristic of material, there are some limitations to using this method for non-homogenous materials. The results of DIC method rely on the speckle pattern on the surface of sample so that a suitable pattern reduces the error of this method. A non-uniform material like the thin interface of biomaterial limits a good speckle pattern on its surface. Moreover, the displacement of the sample in the 2D system during loading is out of plane for a non-homogenous system such as a roller fiber[26].

1.6 Motivation and long-term goal

The motivation of this thesis is to employ DIC method on a non-homogenous system for understanding its deformation characteristics to improve the design of implants and the design of total knee replacement system. The goal of this study is to develop the autotomized computational technique to measure deformation characteristics of versatile materials with varying material properties. This will be useful for the development and design of orthopedic biomaterials.

1.7 Goals and objectives

The goal of this study is to evaluate the mechanical response due to the applied load by the DIC method for a non-homogeneous system. DIC method was applied to three different non-homogeneous systems: metal-cement, bone-cement and multi-layers' fiber cloth.

The objectives of this thesis are as follows: (1) One objective is to measure the strain at the interface of aluminum and cement by using DIC method. In order to understand the deformation characteristics, a series of images were taken by high speed camera. Using a Matlab program of DIC method, the full-strain at the interface was found. (2) Another objective is to find the full- strain at the interface of bone-cement-aluminum in a knee replacement surgery. (3) The third objective is to find the strain of the rolled fiber cloth that can be used for biomedical applications.

1.8 Organization of the thesis

In chapter 1, DIC method is introduced, along with background and history. The motivation and objective of this study is explained. The execution process of the correlation of the digital images is presented. In chapter 2, the DIC method is applied to find the strain at the interface of the aluminum/cement/aluminum when the load tension is applied. In chapter 3, the DIC method is applied to find the strain at the interface of the bone/cement/aluminum for the compressive oscillating load. In chapter 4, the strain for a non-homogenous system, roller fiber, is determined by DIC method. In chapter 5, the conclusion and future work are mentioned. In Appendix A and B, the materials and devices are presented, respectively. To be familiarized with the DIC method, the conducted preliminary studies are presented in Appendix C as well as the

explanation of procedure of DIC method in Matlab. To compare the DIC method, one of the traditional methods, i.e., strain gauge experiments is conducted and explained in Appendix C. An example of comparing the results of strain in DIC with the mechanical of materials theoretical values in Y axis at the interface of aluminum and cement is presented in Appendix C.

CHAPTER 2

STRAIN FIELD MEASUREMENT OF A BI-MATERIAL BY DIC METHOD

2.1. Abstract

The mechanical characteristic of a non-homogenous system is interested to science. Since the non-homogenous system has the different composition, shape, and texture, it is complicated to find its mechanical properties. In general, the methods using for homogenous system are not productive for a non-homogenous system. One of the scientific values of DIC is the measurement of strain field of a non-homogenous material. For example, the interface of cement and implant that is important in replacement of bone in human body due to diseases. The goal of this study is to examine DIC to find the strain at the interface of cement-aluminum when it is under the influence of tension force.

2.2 Introduction

Since the traditional method like strain gauge is not a proper method for this objective, the DIC method is used in this study. For many application in engineering, the length change is the range of 10^{-5} mm/mm that has tend to the development of different algorithms with the very low systematic error and high resolution. The advances in technology, computer, and software have led the using digital image correlation more often. In this method, the displacement of some points will be measured by tracking a series of captured images by high speed camera of an object before and after deformation. Displacement and strain are calculated by correlation algorithm.

In this study, three experiments are selected as the preliminary experiments to employ the DIC method and to check its results by other experimental methods or theory.AS discussed, the DIC method is based on a mathematic theory and performs by a Matlab program, so it is necessary to verify all results with conventional method as strain gauge or theory behind the experiment. Three chosen experiment in this study are (1) applying the program for the same images (2) applying the program for a piece of Aluminum in compression (3) applying the program for a piece of Titanium in compression. The results experiments (1) and (2) are compared with the theoretical results and experiment (3) checked with the result of strain gauge method as presented in Appendix C. The first step is to familiarize with the dependent and independent variables, such as, resolution of pixel, the random pattern, and the size of the subset in DIC method. The strain gauge method is used to validate the result of DIC method.

2.3 Materials and Methods

2.3.1 Experimental Design and Modelling

In Figure (2-1)[27], the principle of measurement is shown with a subset of sample before and after deformation. The coordinates of all pixels will change after deformation, for example, P and Q are two points in original subset in x-y coordinate whereas P* and Q* are the new position of P and Q after applying load. To obtain the displacement of point Q, a reference subset, (2n+1) * (2n+ 1) pixels, is chosen around point Q in the un-deformed image. The coordinate of Q*(x*, y*) is determined by two equations, (2.1) and (2.2), that Δx and Δy are horizontal and vertical distance from the center of the subset to the point Q (x, y) in original subset.

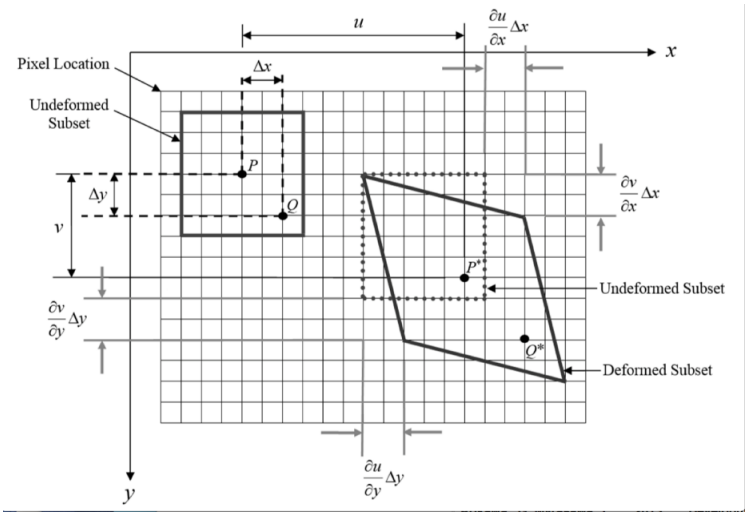

Figure 2.1: The 2D parameters of a subset before and after deformation. Retrieved from [16].

Displacements of the center (p) in X and Y direction are u_x and u_y, respectively. Thus, the coordinates of Q*(x*, y*) can be expressed as:

$$x^* = x + u + \frac{\partial u}{\partial x}\Delta x + \frac{\partial u}{\partial y}\Delta y \qquad (2.1)$$

$$y^* = y + v + \frac{\partial v}{\partial x}\Delta x + \frac{\partial v}{\partial y}\Delta y \qquad (2.2)$$

The parameters, $u, v, \frac{\partial u}{\partial x}, \frac{\partial u}{\partial y}, \frac{\partial v}{\partial x}$, and $\frac{\partial v}{\partial y}$ are controlled to find the subset in the deformed image that match to the subset in the base image.

The cross correlation is applied to evaluate the similarity between the two selected subsets before and after deformation where will be the maximum amount. As discussed in 1.2.2,

different algorithms were introduced to correlate images that Normalized Cross Correlation, NCC, and Zero- Normalized Sum of Squared Difference, ZNSSD, are explained.

The two pieces of aluminum, bonded by cement, is placed in TestResources machine to apply tension. Figure C.4 shows the setup of this experiment. The following sections explain the materials, procedure, and results with analysis of the result

2.3.2 Measurement Approach

I. Algorithm

As discussed in the introduction, the objective of Digital image correlation is to find the deformation and the full-field-strain for a sample during deformation. For this purpose, a program in Matlab is used in this study that has nine .m files and can be downloaded in MathWorks website[28]. This program has written by Chris Eberl *et.al* [29] at the Johns Hopkins University in Baltimore, MD, USA and it is available in website for free. Also, another .m file in Matlab, Cpcorr.m, implements the correlation using NCC algorithm. All steps in running the program will be explained.

II. Determine the base subset of an image

DIC method needs a series of images saved in Matlab and the file of (Filelist_generator.m) generate a folder of a list of images in the current directory in Matlab to process. All images should have TIFF format since TIFF images have a large file size and in processing image they save a lot of detailed image data.

The second command, grid generator, allows you to create the grid in the first image, base image. Then, the x-position and y-positon will be saved in grid_x.dat and y_grid.dat

respectively as a text format. In this step, the subset size is chosen from 10× 10 to 100×100 that determined the resolution of grids. As discussed in Speckle pattern, the subset size is one of the important parameters in the accuracy of the results in DIC method. In this study, different subset size checks for each experiment to find the best resolution depending on the speckle pattern and the size of selected raster.

III. Implementing the correlation

Based on the stated basic concept of correlation above, the Matlab code is used to correlate a series of images before and after deformation. In this study, the concept of Normalized 2-D Cross Correlation has been programmed in the Matlab code, Cpcorr.m, to find the match subsets in two sequence images. For correlating process, the command, automate_image, opens the base image, first image, with the selected raster in grid_generator as green dots then the Cpcorr.m start correlating through all images using Incremental DIC explained in the history of DIC algorithm. At the end, the code writes validx.mat, validy.mat, validx.txt, and validy.txt.

IV. Finding the deformation and full-field –strain in Matlab

Displacement analyzes the taken data from correlation, validx and validy, to find strain and the displacement during deformation. In this step, first validx and validy are loaded then the size of the data is defined finally, the displacement and the full-strain are calculated by the Matlab.

2.4 Experiment

2.4.1 Materials

The materials in this experiment are:

(1) Two piece of aluminum with the length 50.35 mm and the diameter of 12.97 mm.

(2) Cement (PolyMethyl MethAcrylate, PMMA): A veterinary bone cement of Bio Medtrix company: it is radiopaque with low viscosity.

(3) All the apparatus' are mentioned in **Appendix C.2.2**.

2.4.2 Sample Preparation

A piece of aluminum is cut by a diamond machine saw in two half pieces. A laser machine applies the grooves on the one cross section of each sample. The speckles are applied on the outer surface of pieces as discussed in Appendix C.2.1.

2.4.3 Experimental Protocol

The two pieces are placed in the upper and bottom grip of TestResources machine. The target distance of two grip is recorded so that there is a gap of 2 mm for the cement between the two pieces. The distance between two grips are increased to put the cement easily. The amount of 0.4 g of powder of Polymethyl methacrylate/co-polymer is mixed with 200 ml of the liquid Monomer. Methyl methacrylate is placed on top of the bottom sample. The target distance is set up for desired distance and with applying stroke in decreasing distance a force of 38 N applied on the top of cement surface. The cement needs approximately 30 minute to dry. Figure 2.2

shows these procedures. Starting at 50 N, force is gradually increased at a rate of 1N per second. At every 10 N intervals, the camera takes an image and saves the images in a file on laptop.

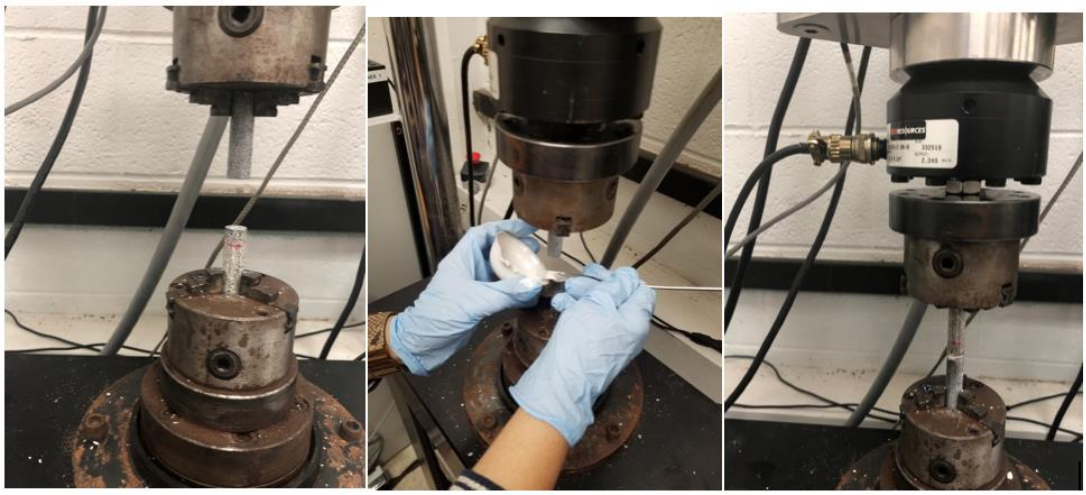

Figure 2.2: (left) two aluminum rods placed perpendicularly at a distance apart; (center) inserting the cement between two aluminum; (right) compression of the cement

2.4.4 DIC model execution

All captured images during the experiment was saved in a series of files and saved in the same folder where DIC algorithm was placed. The four letter of the name of images should be the same to determine a series started with 1 for example “PIC1”. The DIC model starts to make a file of images in order of deformation. Then, the command, grid _generator, opens the first image before deformation to create a subset. In the next step, “cpcorr.m ” in Matlab calculates the correlation coefficient to find the P* and Q*, the position of P and Q after deformation, respectively. With all gathering information, finally, the displacement and strain will be calculated.

2.5 Results and Discussion

This experiment repeats for three times and the results are approximately the same and the cement is broken between 270-280 N. All images are saved in Matlab path and DIC method is run to find the deformation. In the command of grid_generator, the two points at the interface of cement and aluminum are selected to find the strain. The strain of each image for two selected points is plotted in the command of displacement as shown in Figure 2.3:

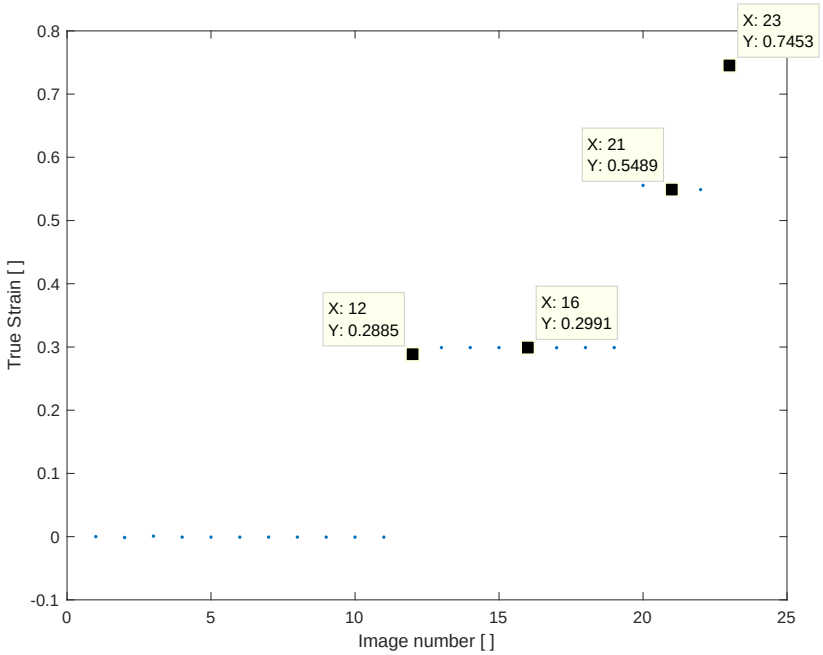

Figure 2.3: The strain in DIC method at interface of aluminum- cement

The definition of strain is used to compare the results of strain in DIC with the mechanical of materials theoretical values. Using the command of Matlab, ‘imshow’, the image 1 in the current file in Matlab will be opened. This image is maximized 3 times and two specific dots are

selected. The coordinates of selected points in pixels are recorded. The other images are opened and after maximizing the coordinates of determined points are recorded as shown in Figure 2.4:

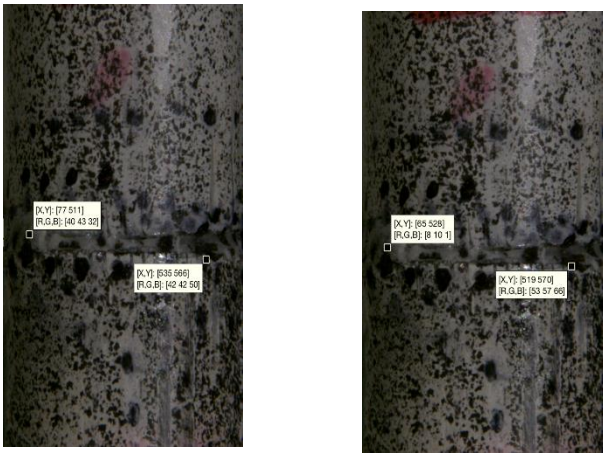

Figure 2.4: (LEFT) Two selected points in the first image (RIGHT) Two selected points in the image number 16.

These coordinates are used to find the theoretical values of strain for each image by using the equation (C-1). One of the sample of calculation is shown in Appendix C.3.3.4. In the Table 2.1, the calculated strain, the strain in DIC method, and percent difference are presented for four images. The Y coordinate of selected points in image 1 are (528,570), so the Y distance between these points is 62.

Table 2.1: The calculated strain theoretically, strain in DIC method, and percent difference.

Image Number	Y_C (pixel)	Y_D (pixel)	L_{DC}(pixel)	Strain Theoretically	Strain DIC Method	% difference of Strain
12	512	565	53	0.2619047	0.2885	9
16	511	566	55	0.30900	0.2991	3
21	498	560	62	0.47619	0.5489	14
23	490	560	69	0.66666	0.7453	11

This validation method is applied for some red marked points in the repeated experiments and the percent error was mostly between 3 and 11 percent. For this experiment the tip of a needle and red ink is used to add the two dots. To get the more accurate results, a needle with a very thin tip is recommended.

2.6 Conclusion

This study successfully calculated strain at the interface of aluminum and cement that is as a non-homogenous system. The first image, the base image, was taken for zero load. The second image was taken where the tension load of 38 N was applied on the sample. The strain of this case was set for zero in DIC program. The next forces were 50N – 150N in tension whose strain are so close to zero. At the 160 N, there is a jump for strain to 0.2885. The next jumps for strain happens at 240. The maximum jump occurs at 270 N with the strain equal 0.7453 where the cement was broken. Although the recorded of displacement by machine was fluctuating, the total displacement from 38 N to 270 N approximately was 0.041 mm. This experiment repeated for two pieces of aluminum without grooves and the cement was broken at 127 N. The different

results of sample with grooves and without grooves is not interested in this thesis, but it can be researched in the future.

The interface at cement-aluminum is considered as a non-homogenous system. One of the mechanical properties of this interface is strain due to applied load as tension. Since the interface is so thin, the introduced DIC method in this study is so accurate to find the strain at interface. Each jump of the value of strain can be determined a significant force that can reduce bounding between cement and aluminum. This information is provided by DIC method may be used to design the implant and cement.

CHAPTER 3

THE STRAIN AT THE INTERFACE OF BONE-CEMENT-ALUMINUM USING DIC METHOD

3.1 Abstract

The PolyMethylMethAcrylate (PMMA) cement bounds the bone and implant and the de-bonding is one of the most concerns in literatures[30]. The continuous strain on the bone – cement-implant is reported as one of the factors of the de-bounding. The de-bounding causes implant loosening at the interface of cement and implant. To solve the de-bonding requires the understanding of bone-cement-implant interface properties in order to the problem. One of the important properties is the deformation characteristic such as strain. There are various methods to determine the properties, such as strain gauge, but none of them are simulation-based and cannot determine the strain at the interface of two different materials. Strain gauges are also limited by the temperature, environment, fatigue and force. This makes it difficult to have an ideal setup. Applying DIC method to find the deformation characteristic like strain at the interface of bone-cement is interested in this study. The result of this section can be used make proper selection of biomaterials in such a way that crack can be prevented at the interfaces.

3.2 Introduction

The DIC is a simulation-based method that can be implored to determine strain at the interface of two different materials, such as bone-cement-aluminum. Since the daily force that acts on the knee of a living human/animal is similar to a compressive oscillating load, the sine pattern for force is considered to apply on a sample of bone-cement-aluminum. The deformation

of sample under the influence of cyclic loading is small. As mentioned in section 2.2, the DIC method is more accurate to find the strain of this sample. The layer of cement is thin, so the resolution of the image can be adjusted or the two markers can be selected to find the strain only at the interface.

3.3 Materials and Methods

3.3.1 Experimental design

The principle of measurement in DIC method is used to modeling in the method of this section as discussed in 2.3.1. The NCC algorithm is sufficient to correlate the selected subsets because the intensity of the deformed subset in this experiment is not too different from the original subset. The two markers are selected to analyze the special part of the sample at interface. The graph of x-displacement versus x-direction is plotted for each image. The curve fit for a linear function is used and the slope of the line is the true strain for each image.

3.3.2 Material

1) A dog bone
2) A designed piece of aluminum for the base of sample:
3) A designed piece of aluminum as an implant
4) A designed piece of aluminum to place on the top of the implant
5) A bag of ‘Plaster of Paris’
6) All apparatuses in section Appendix C.2.2.

A. Sample

Three pieces of aluminum that are designed by Sama Desmond, the graduate student in University of Central of Oklahoma, are connected together as shown in Figure 3.4. The black speckles apply on the surface of the bone-cement-aluminum as explained in chapter 2.

B. Experimental Protocol

The sample with the three pieces of aluminum are placed in the TestResources machine as shown in the Figure 3.2.

Figure 3.2: Set up the sample in the Test Resources machine to apply the compressive oscillating load.

The machine is set for a compressive oscillating load with the amplitude of 30 N and the average of 150 N. This experiment is run for 10^5 cycles with the rate of 1 cycle per second. The setup the program is shown in Figure 3.3

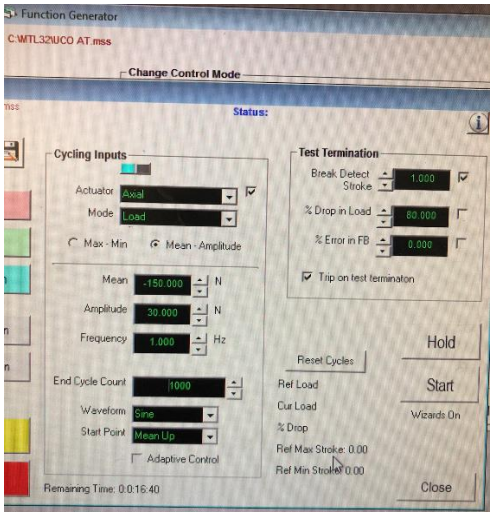

Figure 3.3: The setup the compressive oscillating load in Test Resources machine.

The camera and light sources are placed as explained in the section Appendix C.2.3 to take the digital images. The camera captures image at no load, at 1, 11000th cycle, 21000th cycle, and 27000th cycle and saves in a file in the laptop. One taken image is shown in figure 3.4. The sample of bone-cement-aluminum is placed in the TestResources machine and a compressive oscillating load is applied on the surface of the aluminum. The machine is setup for 10^5 cycles with the rate of 1 cycle per second and some images are taken during the experiment. The DIC program is applied for images to find the strain at interface of bone- cement. The following sections explain the material, procedure, and the results.

Figure 3.4: Captured image of bone-cement-aluminum by camera in compressive oscillating load.

C. DIC model execution

All images are saved in Matlab as a series of images. As discussed in section 2.4.4 the four letters of the images name should be the same. Since the cross section of bone is not fat, the best choice of grid in the base image is 'Two markers'. The two markers are selected at the interface of cement-bone. The images are correlated successfully to obtain the deformed subset match with one in the first image. In the last step, the full-field –strain is calculated in the displacement command.

3.4 Results and Discussion

All images are saved in Matlab and DIC program applied to find the strain at the interface of bone cement-aluminum. The two markers at interface are selected in grid_generator command. The graph of strain versus number of images is shown in figure 3.5.

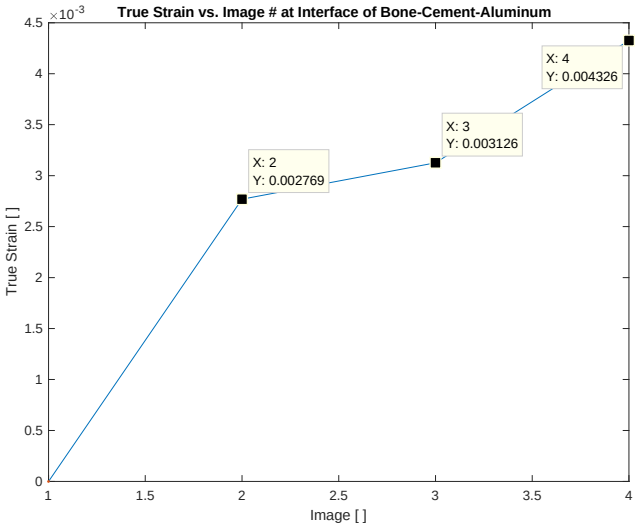

Figure 3.5: The strain vs. number of images at interface of bone-cement-aluminum in compressive oscillating load.

The figure 3.5 indicates that with increasing the cycles, the strain will be increased.

The result of DIC method is compared with the computer program, ANSYS Workbench. The Figure 3.6 shows the strain versus solution calculated by computer program.

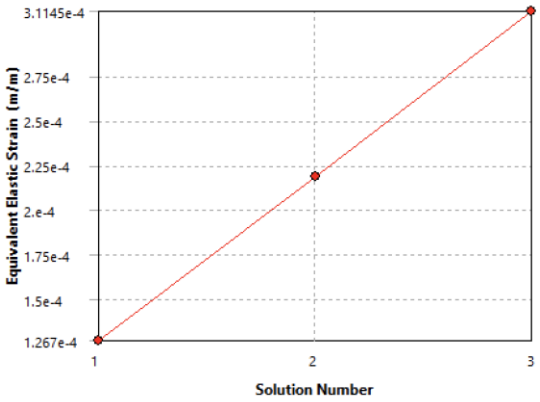

	Equivalent Elastic Strain (m/m)	Change (%)	Nodes	Elements
1	1.267e-004		236868	138154
2	2.1866e-004	53.253	262019	155053
3	3.1145e-004	35.008	311826	189630

Figure 3.6: The Strain versus solution number of bone-cement-aluminum in compressing oscillating load

3.5 Conclusion

The DIC protocol developed in this study can be used to measure the properties of the materials around the interface of two bi-materials. The DIC method is the improved method to find the strain at the interface of bone cement-aluminum. The procedure of DIC method is more practical and accurate compare with traditional methods.

CHAPTER 4

STRAIN FIELD MEASUREMENT OF NANO-FIBER MATRIX WITH DIC

4.1 Abstract

Multi-layers' fiber cloth is a non-homogenous whose composition, shape, and texture are not the same throughout it. The established methods are not improved to find the strain for such a non-homogenous material. This study introduced DIC method to find the deformation characteristics of roller fiber that was obtained from the existing electrospinning system. The fiber can be used for biomedical applications.

4.2 Introduction

In this chapter, the DIC method is run for digital images of a roller fiber. First, the procedure of producing fiber cloth is presented to show how it is considered as a non-homogenous system. The special shape, size, and texture of the fiber cloth are the point of convincing of using a non-contact method, DIC, as the best way to find its strain due to the deformation. An improvement of DIC is to be needed to overcome of the problems of using DIC, mentioned in 1.5.

4.3 Materials and Methods

4.3.1 Materials

1) 0.5 gram of PCL (polycaprolactone)
2) 5grams acetone
3) Syringe
4) Regulated high voltage generator
5) Arduino Uno microcontroller and Arduino IDE

6) Stepper Motor
7) Stepper driver
8) Rotating Drum
9) Potentiometer
10) A 32mm roller fiber was made in this study

4.3.2 Fiber Production

There are several steps to generate the nanofiber on a roller drum. First, 0.5 gram of polycaprolactone (PCL) with 5 grams of acetone is mixed to create PCL solution. The syringe is filled with the solution. The nanofiber is collected by the electrospinning method—electric charge produced by a high voltage generator to attract threads of the polymer solution that is leaving the syringe needle. The specific rate of flow from the syringe pump is programmed to be continuous. The syringe pump system consists of a stepper motor, stepper driver, regulated power supply, and Arduino Uno microcontroller. The collector is a rotating metal drum.
The Arduino is programmed to supply a drop of the PCL solution every second. The steps of the stepper motor are divided equally into 360° (full rotation). The stepper driver controls the amount of current that runs through the motor and the modes of rotation. The potentiometer limits the current that is going into the stepper motor. The regulated power supply converts the alternating current into direct current.

4.3.3 DIC Execution

The modeling and algorithm are the same as selected in chapter 2. Since the extension of the fiber due to a tension is large, the way of choosing the grid in the base image will be changed. In the grid_ generator, the rectangular area is selected approximately in the middle of

the base image. The Implementing of the correlation and finding displacement are the same as the one in chapter 2.

4.3.4 Experimental Protocol

A roller fiber is divided in to three equal pieces to apply tension by TestResourses machine.

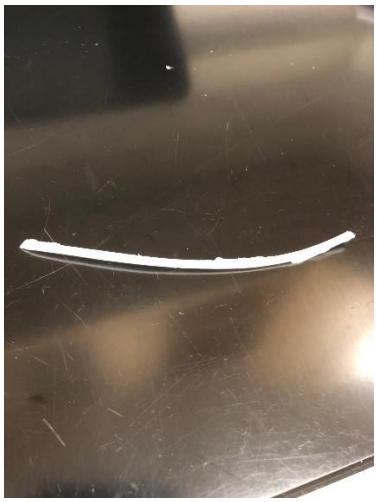

Figure 4.1: The piece of roller fiber.

The set up the experiment is the same as the experiment in chapter 2 as shown in figure 4.2:

Figure 4.2: Experimental Set-up of Roller fiber

Digital camera takes images to use DIC method. This experiment is repeated 3 times. The black speckles are applied on the surface of roller fiber. The roller fiber is placed in the TestResources machine. The length of roller that is outside the grips is 32.0 mm. The distance between two grips is increased gradually by 1 mm. Although the magnitude of force is fluctuating, the force is recorded approximately between 2 N to 26 N that the piece of fiber is broken at 26 N with the total displacement about 30 mm. An image is captured for every 1 mm increment.

4.4 Results and Discussion

The DIC method is applied for images. Since the length of roller is increasing, the best option in DIC method to find the displacement is True-Full-filed strain. The subset is used for the middle of the roller's length. The result is shown in figure 4.1:

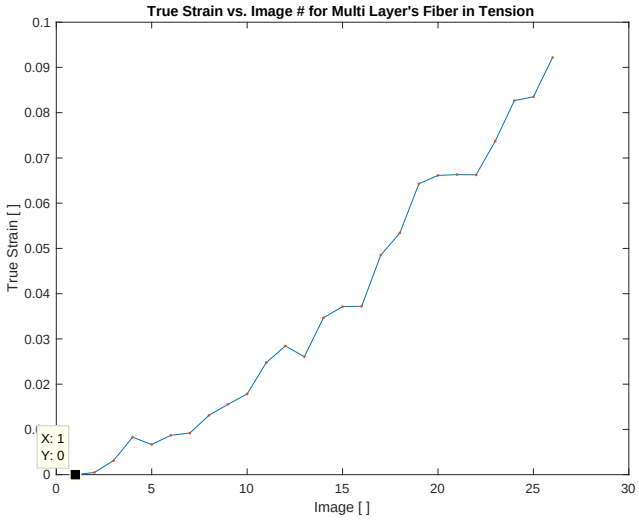

Figure 4.1: The strain of roller fiber in tension for every 1 mm increment of increasing length.

This experiment is repeated 3 times to the results are reproducible. For each experiment the fiber is broken at 49N -50 N with the total displacement of 30 mm.

All strain in DIC method are recorded and with the values of force and the area of roller, the stress is calculated.

Most researchers determine the relationship of the stress-strain with the help of curve fitting. In this method, a smooth function is constructed to fit a measured series of data point. The value of regression analysis, R^2, determines the best fit of the curve. The relationship between stress and strain is shown in figure 4.2:

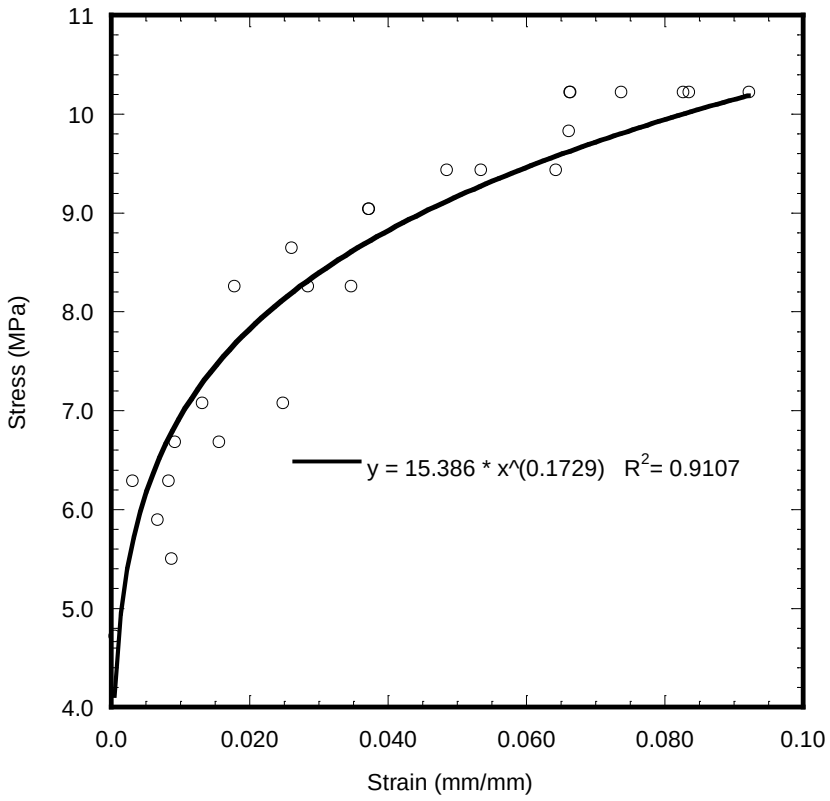

Figure 4.2: The stress versus strain for a multi-layer' fiber in tension Load.

As R^2 value of this graph is 0.91, which is closest to the ideal value ($R^2 = 1$), the relationship between stress and strain is the equation (4.1):

$$\sigma = 15.386\ \epsilon^{0.1729} \tag{4.1}$$

The stress is related with the strain with a power function. For the used fiber in this study, the coefficient is 15.386 (MPa) and the power is 0.1729.

4.5 Conclusion

In this study, the DIC method was developed to find the true full -field - strain for one example of non-homogenous material, multi layer's fiber. Since the strain of this material is not proportional to length increment, the tradition method is not compatible to calculate the strain of

roller drum nanofiber. The procedure of DIC method is more practical and accurate in comparison to the traditional methods. In this study, a power function is presented to show the relation between stress and strain for a multi- layer' fiber, $\sigma = m\epsilon^{k}$. The coefficients of presented equation are determined by the properties of fiber.

CHAPTER 5

CONCLUSION AND FUTURE WORK

5.1 Conclusion

In this study, three non-homogeneous biomaterial interface surfaces were considered. For the aluminum-cement case, the deformation characteristics, for example, strain, were found when the cement was broken from applied tension. These characteristics can help in the design of future implants and the composition of cement. For the bone-cement-aluminum case, a compressive oscillating force was applied to the aluminum in order to simulate the everyday tension on the knee of a living human/animal. The results from this study can help in the development and design of orthopedic biomaterials by ensuring that the materials are strong enough to withstand forces applied to a knee. Lastly, with the multi-layers' fiber cloth, the DIC method was used to find the mechanical properties of the fiber, though this method is not suited for non-homogeneous surfaces. As a result, a power function is presented to show the relation between stress and strain for a multi- layer' fiber, $\sigma = m\epsilon^k$ values for strain for the fiber cloth.

5.2 Future work

The DIC method should be improved to find the strain at a localized interface of two sufficiently large regions. This limitation of the DIC method has restricted the strain measurements in two of the results in this study. Currently, the correlation coefficient of the images in these two results cannot be evaluated due to this issue. As a result, the strain cannot be calculated. Either we can determine a way to correct for this image resolution problem within the

DIC method itself, or we can change the way in which we collect images. One possibility in changing the way in which images are collected is by changing the method of speckle pattern creation so that the DIC method can detect subtle changes in successive images.

APPENDIX A

LIST OF MATERIALS

1) Two pieces of aluminum with the length of 46.25 and diameter of 12.97 mm and Elastic modulus of 6.9×10^{10} Pa

2) A Cantilever Beam: An Aluminum cantilever beam with the length of 195 mm. The beam has a rectangular section of 2.28 mm height and 10.64 mm width. The Elastic modulus of beam is 6.9×10^{10} Pa

3) A clamp and some weights 20, 50, 100, and 200 g with the 50 g hanger.

4)A digital Vernier Caliper: a Vernier Caliper with a precision of 0 .01 mm: a Vernier Caliper with a precision of 0 .01 mm

5) Super glue: a super glue made by Omega

6) Acetone

7) Tweezer

8) A cylindrical Piece of Titanium Ti-6Al-4V with the length of 78.95 mm and diameter of 9.54 mm. The Elastic modulus of beam is 19.3×10^{10} Pa

9) A veterinary bone cement of Bio Medtrix company to make cement it is radiopaque with w viscosity**.**

10) An artificial dog bone

11) A designed piece of aluminum for base of sample:

12) A designed piece of aluminum as an implant

13) A designed piece of aluminum to place on the top of the implant

14) A 53mm roller fiber

15) A bag of ‘Plaster of Paris’

APPENDIX B

LIST OF INSTRUMENTS AND SOFTWARE

B.1 All instruments have been used in this study are shown in Table B.1:

Table B.1: The information of all instruments and software.

Device and software[31]	Company	Model	Feature
Digital Camera[31]	Phantom	V641	2560 *1600 maximum resolution
Matlab	MathWorks	R2017b	64 bit
Strain Gauge	Omega	-	351.2 Ω ± 0.35 % Ω Gage factor = 2.04 ± 1.0 %
TestResoursec machine	-	-	-
LabVIEW	National Instruments	2016	64 Bits
Amplifier	Omega	DMD-465 Bridgesensor	Output Voltage = 4 to 15 volts

APPENDIX C

THE PRELIMINARY EXPERIMENTS AND CALCULATION OF PERCENTAGE ERROR

C.1 Running the DIC Program for the Same Images

C.1.1 Procedure and results

The first test is to find the correlation of a series of duplicated images and to find the displacement in 1D system. It is obviously clear that the displacement should be zero for the same images. The Figure C-1 shows the positions of two selected markers after correlation in the same five images. Each column presents the X-Position in pixel of two markers in one image. Since there is no difference between images, the coordinates of each point should be equal and the results show the accuracy of DIC program.

```
>> automate_image

ans =

   68.9640   68.9640   68.9640   68.9640
  265.0020  265.0020  265.0020  265.0020
```

Figure C.1: The positions of two markers in pixel for four copies of one image.

The displacement of pixels with the subset size 50×50 is shown in Figure C.2:

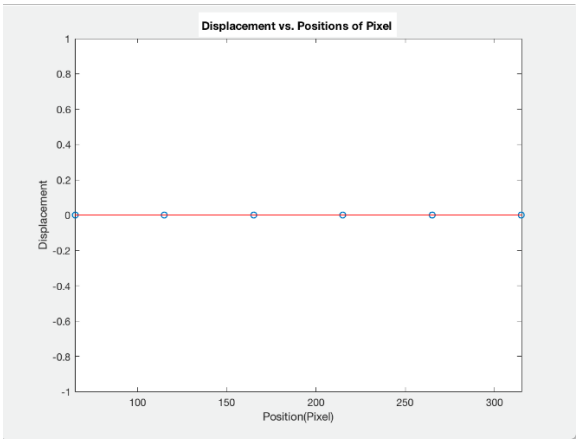

Figure C.2: The displacement of pixels for four copies of one image.

The displacement of two pixels is zero in entire images.

C.1.2 Conclusion

The simple way to validate DIC method is running the program for some copies of one image. In this paper, two points in 5 copies of one image were correlated and the results shows the program well correlated and the result of displacement well validated Matlab program to perform DIC method.

C.2. Running the DIC program for a piece of aluminum in compression

A piece of Aluminum in compression uses to perform DIC program in this study as a real preliminary experiment. The equipment and procedure will be explained in the following sections.

C.2.1 The Preparing the Sample

The specimen is a cylindrical rod of Aluminum with the length of 46.25 mm and diameter of 12.97 mm to run the experiment in this section. The surface of the rod should contain a random pattern as discussed in speckle pattern. Therefore, White and Black spray paint applied the pattern on the surface of rod. A coat of white paint applied of the whole surface of sample then the random black speckles sprayed on the bar from the approximately 1 m above its surface as shown in Figure C.3:

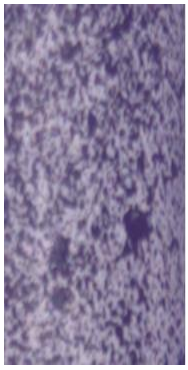

Figure C.3: The specimen with the applied speckle pattern.

C.2.2 Experiment Apparatus

The experiment is set up with all devices as shown in Figure C.4:

Figure C.4: The set up the experiment of a piece of Aluminum in compression.

The following section will present all information about each apparatus

1) Digital Camera: the digital camera in this experiment is a Phantom V641 (as shown in Figure C.5) with a high resolution. A digital camera[32] save images electronically with a series of numbers that can be edited.

Figure C.5: The digital camera Phantom V641.

With pressing the button to take a photo, the light converges in to the lens of camera. This picture hits a sensor chip that converts the image to millions of pixels. The color and brightness of each pixel in picture are measured and stored as a number. The digital camera can connect to a computer and digital images can be downloaded and load in any digital devices. The V641 is 4-megapixel with the resolution from 1920×1080 to 2560×160 and 35 mm field of view at full resolution. Its frame rate is from 10 to 2560 fps and it has CMOS sensor(see[33]). The camera able to save all images in the TIFF format.

2) A laptop computer: a laptop with 64-bit version of Windows 10 supports the software PCC (Phantom Camera Control application) that controls Phantom camera. This software is available in Phantom website.
3) Tri-pod stand: a basic tri-pod stand holds the camera fixed and normal to the surface sample.
4) Light source: two 2500 Lumen Led Portable Work-light illuminate the right and left side of the surface of specimen.
5) Test Resources machine: a loading machine is used for static compression or tension test.
6) Desktop computer: a desktop computer is connected to TestResource machine. An installed software program in this computer controls the machine. This software determines type of load, measures, and saves all the variable in the test.

C.2.3 Experiment Setting

The specimen was placed in TestResources machine and as showed in the set-up of experiment in Figure C.4, a compression test applied on specimen. For this purpose, the option ‘load’ is selected in the machine and the distance between two clamp is adjust to zero load, first. The camera is connected to laptop and the software, Pcc, will be opened to show the captured images by the camera. A new file on the desktop is created to save the images and in the ‘manager’ tap of the software the path of saving images in this file is determined. The camera should be placed in front of the sample, normal to the surface of sample. The two sources of light are placed in the right and left of camera. With turning the two lens of camera, a clear image appears on the screen of laptop. The first image is taken by camera with no load. The distance of two grip is changed that the machine starts with -314 N which the negative shows the compression. The second image is taken now. With increasing the load, some images are taken during compression. The applied load was from 314 N to 1040 N with a 1 rate /sec and total displacement measured by the machine was 0.296 mm. 24 images were taken by digital camera with a resolution of 1024×1024 and the sample rate of 50 fps.

C.2.4 Analyzing Results by DIC Method

All 24 images were saved as .TIFF format in Matlab and after creating a file-list of images in directory file of Matlab, the grid for base image was defined. Since the subset size is one of the factors matters in the results of DIC method, different sizes were checked and the results were compared. In Figure C.6, the base image for 50×50 resolution is shown:

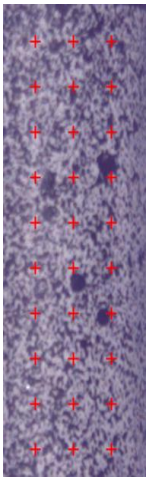

Figure C.6: The base image with 50 × 50 resolution

In running automate_image Incremental , Figure C.7, DIC method tracks image number i to the image number i+1 and a new raster is plotted as red crosses and so on.

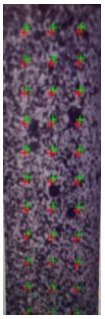

Figure C.7: Correlating image in automate_image command.

The option ‘1D average full strain measurement ‘in displacement command plots strain vs. image number as shown in Figure C.8:

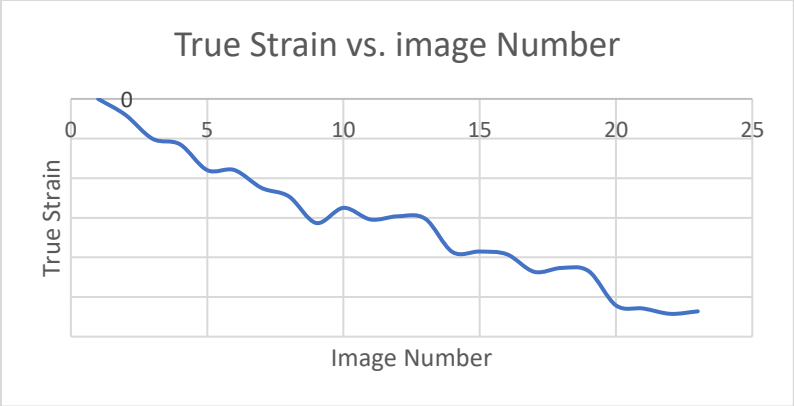

Figure C.8: True strain in Y direction vs. image number

C.2.5 Validating the results of DIC method

The results of DIC method are compared with the calculation based on the classical solid mechanics.

C.2.5.1 The definition of stress, strain, and Elastic Modulus

Tensile stress or compressive stress are defined in physics when a force pulls or compress an object, respectively. The Stress and strain define[34] as equation (C.1) :

$$\sigma = \frac{F}{A} \qquad \varepsilon = \frac{\Delta l}{l_o} \tag{C.1}$$

where F is the normal force, A is the cross-sectional area of the object, σ is the stress, Δl is the change of the object's length, lo is the initial length of object, and ε is the strain.

The stress and strain are in direct proportion in low stress and the Elastic modulus (or Young's modulus) is defined as equation (C.2):

$$Y = \frac{\sigma}{\varepsilon} \qquad \text{(C.2)}$$

Young's modulus is measured for various materials in laboratory and it depends on various physical conditions.

C.2.5.2 Comparing Strain in DIC Method with Calculating from TestResource machine

As discussed in previous section, the stress and strain are in direct proportion for low stress, so the graph of stress versus strain for aluminum should be a straight line. The TestResources machine records the value of force in compression. Therefore, the stress along applying compression on the object was calculated by equation (C.1) and the strain of each image in DIC was found from Figure 3-8 then the graph of stress versus strain was plotted in Figure C.9:

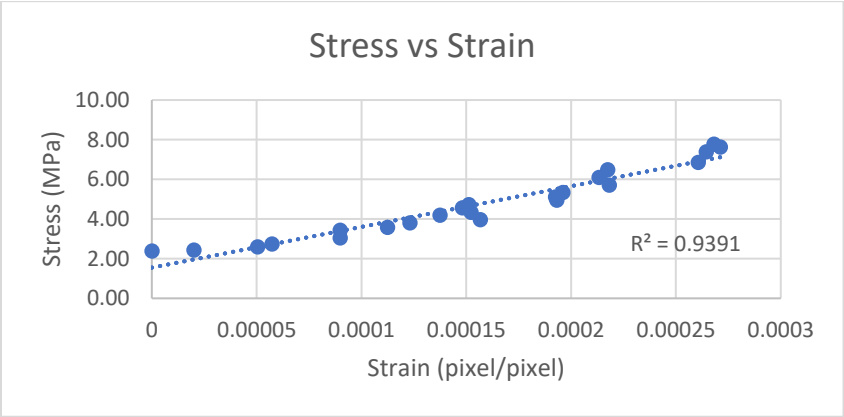

Figure C.9: Measured stress by Test Resources machine vs. strain in DIC for a piece of aluminum in compress

This graph is approximately a straight line using the best fit curve in excel, and R^2 is close to ideal value, 1. The factors affecting the error in this trial are misalignment of TestResources machine, the crooked surface of specimen, and uniform lighting on the surface of rod.

C.2.6 Conclusion

In this study, the results of a known experiment in DIC method was employed for a series of images of an aluminum specimen in compression to find full-field strain. The applied stress on the specimen was calculated by the recorded data by TestResources machine. The graph of stress versus strain was approximately a straight line that verified the accuracy of DIC method. This test was employed 4 times to get the best results. The first time, misalignment occurred because of slight local buckling then the speckle pattern did not have a random shape. The two left experiments have the same results. The recommendations to get the better results are to fix the TestResources machine, to select a homogenous specimen with a flat surface, to apply a nice speckle pattern, and to choose the best subset size.

C.3 Running the strain gauge and DIC methods for a piece of titanium in compression

The second experiment in this research is a piece of titanium in compression to run DIC method to find the full- field- strain. In this section, the results compare with the traditional method. For this purpose, strain gauge, and the advantages of DIC compare to strain gauge method will be discussed.

C.3.1 Strain gauge and its application in measuring strain

The strain gauge is an electrical sensor [35] that applied for measuring mechanical quantities. A long, thin strip in zig-zag shape in parallel made of a conductive material is a strain

gauge. The resistance of strain gauge changes with changing of its length by external applied force. The strain gauge is used to measure strain of a specimen in tension or compression. Therefore, the strain gauge is bounded on the surface of specimen by a super glue. If the test specimen experiences the strain, the strain transfers directly to the strain gauge which causes a linear change in the length and the electrical resistance of strain gauge. Thus, strain gauges can be used in measuring strain of a sample in tension or compression. Since the changes of resistance are small, strain gauges are used in a Wheatstone bridge circuit.

In this study, a strain gauge replaced with one of the four resistance in a bridge, Quarter-Bridge Circuit, as shown in Figure C.10 [36]:

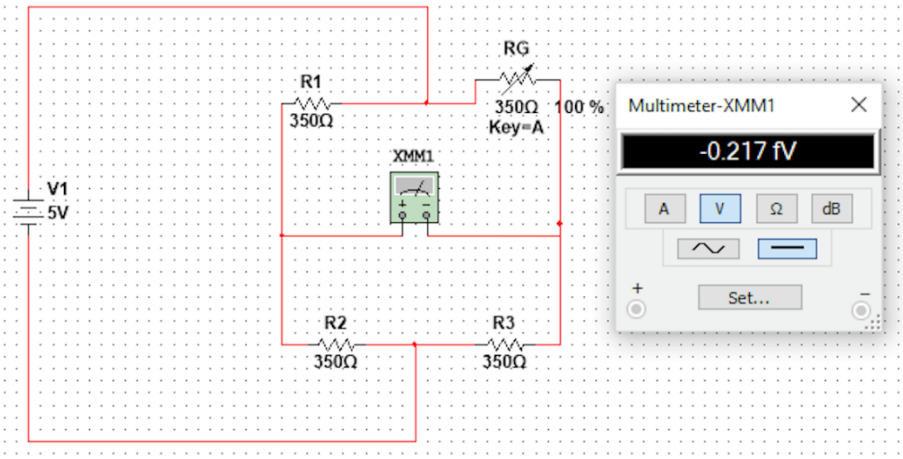

Figure C.10: Quarter bridge circuit.

Since the output voltage, V_o, is too low, an amplifier is used to enhance the output voltage, $V_{amp,}$ with the gain of G in equation (C.3).

$$G=\frac{V_{amp}}{V_o} \qquad \text{(C.3)}$$

The output voltage of Wheatstone bridge, V_o, is given by the equation: (C.4):

$$V_o = \left[\frac{R_3}{R_G+\Delta R+R_3} - \frac{R_2}{R_2+R_1}\right] V_s \qquad \text{(C.4)}$$

that V_s is excitation voltage. For equal initial resistances, V_o is simplified to equation (C.5):

$$V_o = \frac{\Delta R}{4R} V_s \qquad \text{(C.5)}$$

Using the definition of strain gauge factor of strain gauge [17] , equations (C.6), the output voltage is given by the equation (C.7):

$$S = (\Delta R/R)/ \varepsilon \qquad \text{(C.6)}$$

$$V_o = \frac{\varepsilon S}{4} V_s \qquad \text{(C.7)}$$

where S is the strain gauge factor and ε is strain factor of sample which defines as $\frac{\Delta L}{L_o}$.

Using equations (C.3) and (C.7), the strain factor gain from equation (C.8):

$$\varepsilon = \frac{4\, V_{amp}}{GSV_s} \qquad \text{(C.8)}$$

C.3.2 Strain gauge test in bending

One of the goal in this chapter is to validate DIC method with strain gauge, so it is productive to be familiar with the strain gauge test. Thus, some experiments are designed to find the strain of a sample by strain gauge. One of these experiment is to find strain of a cantilever beam in bending test. In the following section, this experiment will be discussed.

C.3.2.1 The theory of strain for bending test and method

The strain factor of a cantilever beam in bending test [38] is gained by equation (C.9).

$$\mathcal{E} = \frac{6\,F\,L}{E\,b\,h^2} \qquad \text{(C.9)}$$

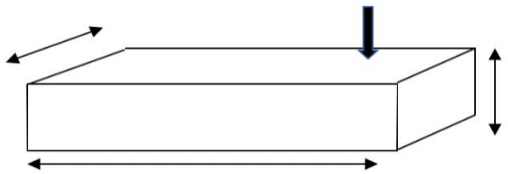

Figure C.11: a cantilever beam in bending test.

As shown in Figure C.15: F= Applied force, L= Length from the center of strain gauge to center of applied force, E = Modulus elasticity, b= Width of beam, h= Height of beam.

In this part, an experiment is set up to find the strain of a cantilever beam in bending test in two ways:

1) by reading voltage of a quarter bridge and using equation (C.8)

2) by measuring applied force and using equation (C.9). An Aluminum cantilever beam is equipped by strain gauge which is glued at the one end of beam on its surface. One end of cantilever beam is attached to a rigid support and the other side of beam is free. The strain gauge connected to a Wheatstone bridge. The load is applied in the free side of the beam. The calculated strain in two ways should be equal.

C.3.2.2 Experiment Apparatus

Figure C.12 shows the experimental setup.

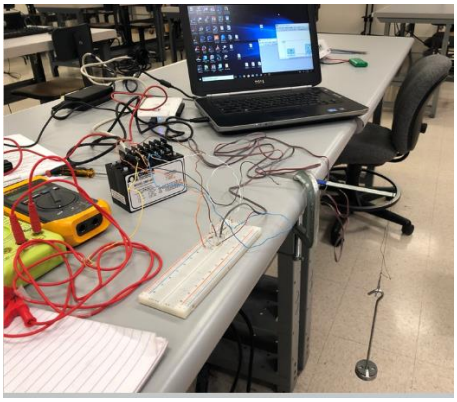

Figure C.12: Experimental setup in bending test

The apparatus consists of:

1) A Cantilever Beam: An Aluminum cantilever beam with the length of 195 mm. The beam has a rectangular section of 2.28 mm height and 10.64 mm width.
2) Loading Fixture and Weights: a clamp and some weights 20, 50, 100, and 200 g with the 50g hanger
3) Strain gauge: a strain gauge is manufactured by Omega Engineering, Inc., Stamford, CT. Figure C.13. The resistance of strain gauge is 350 Ω and gauge factor of 2.04.

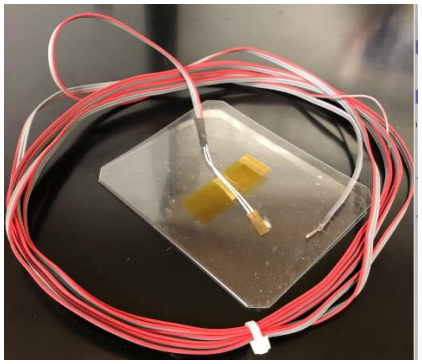

Figure C.13: The strain gauge made by Omega Company.

4) Resistors: three equal resistors of 350 Ω
5) An amplifier: a DMD-465Bridgesensor amplifier is manufactured by Omega company. The output voltage of amplifier is from 4 to 15 volts.
6) A laptop with installed LabVIEW: a laptop with 64-bit version of Windows 10 supports the software LabVIEW 64 bits, 2016.
7) NI myDAQ: a data acquisition device that uses NI LabVIEW- based software instrument [39] to measure output voltage.
8) A digital Vernier Caliper: a Vernier Caliper with a precision of 0 .01 mm
9) Super glue: a super glue made by Omega.
10) Acetone
11) Tweezer
12) Cellophane tape

C.3.2.3 Experiment setting

The length and actual cross –sectional dimensions of the beam is measured by a digital Vernier caliper. A distance 13 mm from one end of the beam is marked to attach the strain gauge

on the surface of beam. The desired area for strain gage is cleaned by acetone to make sure it is degreased[40]. A tweezer is used to place it on the cleaned surface. The ribbon leads should face up then a piece of cellophane tape is gently placed on top of the strain gauge. One end of tape is hold on the strain gauge and gently the other end is lifted and a thin layer of super glue is applied on the surface of specimen. The tape is retuned back to the correct position. The surface of tape is pressed for 3 minutes then the tape is peeled back carefully. The Wheatstone bridge is set up as shown in Figure C.14. Then, the beam is mounted to the clamp as shown in Figure C.12. A program in LabVIEW is written to measure the output voltage of the circuit which shown in Figure (3-14):

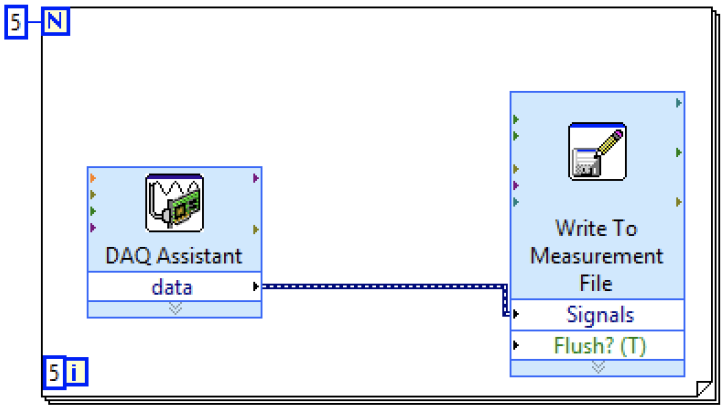

Figure C.14: The LabVIEW program to measure voltage.

The weight from 50 g to 350 g with increment of 20 is hung at the end of the beam and the output voltage will be measured.

C.3.2.4 The results of strain in bending test

The graph of gained strain from equation (C.9) versus the gained strain from equation (C.8) is shown in the Figure C.15:

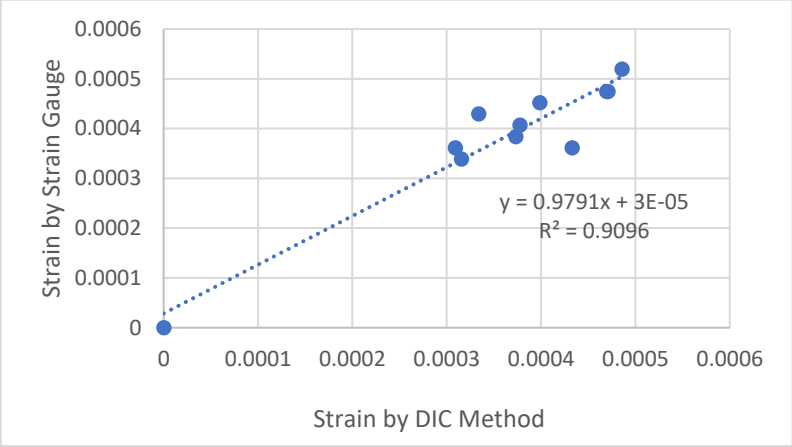

Figure C.15: The theoretical strain versus strain of strain gauge for cantilever beam in bending test

C.3.2.5 Conclusion

The result of bending test validates the DIC method since the graph of theoretical strain versus strain of strain gauge is approximately a straight line with a slope of 1, and R^2 value, using fit curve fit in excel, is close to ideal number, 1.

This experiment experience error such as: the weights are not so accurate, output voltage of amplifier sometimes is fluctuating, the dimensions of rod are not the same along the length.

C.3.3 Strain of a piece of titanium in compression

One of the preliminary experiments in this study is finding strain of a piece of titanium in compression by DIC and strain gauge methods. Titanium is used in this step of this study because it mostly is used as implants in orthopedic and orthodontic surgeries. The alloy of Titanium, Ti-6Al-4V, is better than pure Titanium since it has the better physical and mechanical property for example it does not react with body fluid. Also, DIC method can be compared with the Strain gauge method which is a traditional method in finding strain of metals.

C.3.3.1 Experimental setup

A strain gauge is bounded on the surface of a piece of titanium and connected in a quarter bridge circuit. Titanium is placed in between two grip of TestResources machine. The digital camera is located in front of sample normally to take digital images. The machine is set on load option for compression.

C.3.3.2 Materials

1) A cylindrical Piece of Titanium Ti-6Al-4V with the length of 78.95 mm and diameter of 9.54 mm.

2) A strain gauge 350 Ω and gauge factor of 2.04 made by Omega company.

3) A super glue made by Omega Company.

4) All apparatus' were mentioned in section C.2.2. and C.3.2.2.

C.3.3.3 Procedure

The place of strain gauge on the surface of titanium is cleaned, marked to bound the strain gauge as mentioned in section C.3.2.3. The super glue is applied on the selected place and the strain gauge bounded on the surface. The strain gauge will be connected to a quarter bridge circuit and an amplifier to measure the output voltage of circuit. Then, the sample is placed between the two grip of TestResources machine to apply forces on compression. The camera takes an image for each load as the same mentioned in the section C.2.3

C.3.3.4 Results of titanium on compression

The voltages recorded in LabVIEW program are plugged in equation (C-9) to find the strain in strain gauge method. The DIC method is applied for all taken images as explained in section C.2.4 In displacement command of DIC program, some badly points will be removed from the images. Table C.1 shows some measured voltages and strain in DIC method.

Table C.1: The results of output voltage of circuit, Difference of voltage about initial voltage (v), strain by Strain gauge method, and Strain in DIC method for a piece of titanium in compressing load.

Output Voltage of circuit (v)	Difference of voltage about initial voltage (v)	Strain by Strain gauge method	Strain in DIC method
1.678434	0	0	0
1.847404	0.16897	0.00033862	0.0003156
1.858669	0.180235	0.00036119	0.000309

1.858669	0.180235	0.00036119	0.000433
1.869934	0.1915	0.00038377	0.0003733
1.881198	0.202764	0.00040634	0.0003775
1.892463	0.214029	0.00042892	0.0003339
1.903728	0.225294	0.00045149	0.0003986
1.914993	0.236559	0.00047407	0.0004708
1.914993	0.236559	0.00047407	0.0004695
1.937522	0.259088	0.00051921	0.0004858

The strain by strain gauge has an average of 0.000381715 with 0.000138592standard deviation, and the strain by DIC method has an average of 0.000360636 with the standard deviation of 0.000134998.

The Figure C.16 shows the calculated strain by strain gauge method versus strain by DIC method:

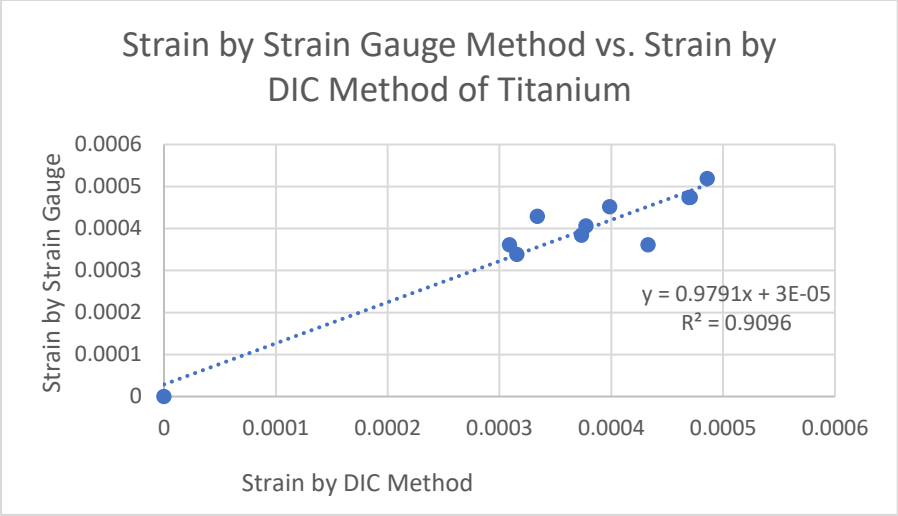

Figure C.16: the calculated strain by strain gauge method versus strain by DIC method.

The slope of this figure is approximately equal 1 that verifies the values of DIC method with the strain gauge method.

C.4 Percentage of difference between strain in DIC and theoretical value

An example of comparing the results of strain in DIC with the mechanical of materials theoretical values in Y axis at the interface of aluminum and cement are presented below:

The points A, and B were selected in image (1) with the Y coordinate of:

A (528), and B (570)

After deformation, point A and B were in the new position C (511) and D (566), respectively, in image 16. The strain is calculated by:

Length of AB in Y axis = L_{AB}

L_{AB} = 570-528= 42

Length of CD in Y axis = L_{CD} = 566-511=55

Strain = $\frac{L_{CD} - L_{AB}}{L_{AB}} = \frac{55-42}{42} = 0.309$

The strain between the selected points in DIC for image 16 is equal 0.2991.

The percent difference was calculated by:

% difference = $\left| \frac{0.309-0.2991}{\frac{0.309+0.2991}{2}} \right| = \%\ 3$

REFERENCES

1. Hobrough, G.L., *The photogrammeric Record.* 2003. **18**(104): p. 337-340.
2. .A, R., *From Image Analysis to Computer Vision: An Annotated Bibliography, 1955–1979.* Computer Vision and Image Understanding, 2001. **84**(2): p. 298-324.
3. Schreier, M.A.S.J.-J.O.H.W., *Image Correlation for Shape, Motion and Deformation Measurements*.
4. Mallick, S.R., M.L, *Speckle-pattern interferometry applied to the study of phase objects.* Optics Communications, 1972. **6**(1): p. 45-49.
5. *HIGH-SPEED IMAGING: Digital image correlation measures 3D surface deformation*. 2012; Available from: https://www.laserfocusworld.com/articles/print/volume-48/issue-09/features/digital-image-correlation-measures-3d-surface-deformation.html.
6. Peters, W.H., Ranson, W.F, *Digital imaging techniques in experimental stress analysis.* Optical Engineering, 1982. **21**(3): p. 427-431.
7. McNeill, M.S.W.W.W.P.W.R.S., *Determination of displacements using an improved digital correlation method.* Image and Vision Computing, 1983. **1**(3): p. 133-139.
8. Sutton, T.C.C.F.R.A., *Applications of digital image correlation techniques to experimental mechanics.* Experimental Mechanics, 1985. **25**(3): p. 232-244.
9. PetersIII, H.A.B.R.M.A.S.H., *Digital image correlation using Newton-Raphson method of partial differential correction.* Experimental Mechanics, 1989. **29**(3): p. 261-267.
10. Hovis, G.L., *Centroidal tracking algorithm for deformation measurement using gray scale digital images.* 1989.
11. Bing Pan, K.L., *A fast digital image correlation method for deformation measurement.* 2011. **49**(7): p. 841-847.
12. Michal Maj, M.T.N., *Determination of coupled mechanical and thermal fields using 2D digital image correlation and infrared thermography: Numerical procedures and results.* 2018.
13. Zhou.Y, C.Y., *Propagation function for accurate initialization and efficiency enhancement of digital image correlation.* 2012.
14. BING Pan, W., Xia Yong, *Incremental calculation for large deformation measurement using reliability-guided digital image correlation.* Optics and Lasers in Engineering, 2012. **50**(4): p. 586-592.
15. Jiang L, X.H., Panb B, *Speeding up digital image correlation computation using the integral image technique.* Optics and Lasers in Engineering, 2015. **65**: p. 117-122.
16. *Pixel*. Available from: https://www.webopedia.com/TERM/P/pixel.html.
17. HANG, Z., *Digital image correlation analysis of a alkali silica reaction in concrete with recycled glass aggregate* 2014.
18. *Speckle Pattern Fundamentals*. Available from: AN1701-Speckle Pattern Fundamentals.pdf (page 1 of 13).
19. Lathi, B.P., Ding, Z, *Modern Digital and Analog Communication Systems*. 4 ed.: Oxford.
20. Lewis, J.P., *Fast Normalized Cross-Correlation*, I.L. Magic, Editor.
21. *Understanding Cross-Correlation, Auto-Correlation, Normalization and Time Shift*. 2016.
22. Pan, B., *Reliability-guided digital image correlation for image deformation measurement.* Applied Optics, 2009. **48**(8): p. 1535-1542.

23. Terry Yuan-Fang Chena, T.-C.C., Fa-Yen Chenga, Ang-Ting Tsaic, Ming-Tzer Linc,d,∗, *Digital image correlation of SEM images for surface deformation of CMOS IC*. 2018: Microelectronic Engineering.
24. Maji, S., *What does homogeneous and isotropic material mean?* Quora, 2015.
25. Pabasara, *Difference Between Homogeneous and Heterogeneous Mixtures.* PEDIAA, 2017.
26. Plalanca, M., Gianluca, T, *The use of digital image correlation in the biomechanical area.* 2015. **34**.
27. Sze-Wei Khoo, S.K., Ching-Seong Tan, *A review of surface deformation and strain measurment using two dimensional digital image correlation.* Academy of Sciences, 2016. **23**: p. 461-480.
28. Eberl, C. *Digital Image Correlation and Tracking*. 2010; Available from: https://www.mathworks.com/matlabcentral/fileexchange/12413-digital-image-correlation-and-tracking.
29. Eberl, C., *Digital image correlation and tracking.* Mathwork, 19 Nov 2010.
30. Wang, X., Agrawal, M., , *A mixed mode fracture toughness test of bone–biomaterial interfaces.* Journal Recommendation service, 2002. **53**(6): p. 664-672.
31. *Phantom v641*. Available from: http://www.adept.net.au/cameras/visionresearch/Phantomv641.shtml.
32. Woodford, C. *Dihital Camera*. 2018; Available from: https://www.explainthatstuff.com/digitalcameras.html.
33. *What is the difference between CCD and CMOS image sensors in a digital camera?* ; Available from: https://electronics.howstuffworks.com/cameras-photography/digital/question362.htm.
34. *Stress, Strain, and Elastic Modulus*. Available from: https://courses.lumenlearning.com/suny-osuniversityphysics/chapter/12-3-stress-strain-and-elastic-modulus/.
35. *What is a strain gauge?* ; Available from: https://www.omega.com/prodinfo/strain-gauges.html.
36. Khandakar, M., *Laboratory Manual for Strength of Materials Lab.* 2014: p. 2-5.
37. Cimbala, J.M. *Stress, Strain, and Strain Gages*. 2013; Available from: https://www.mne.psu.edu/cimbala/me345/Lectures/Strain_gages.pdf.
38. *Stresses: Beams in Bending.*
39. *NI myDAQ USER GUIDE AND SPECIFICATIONS*. Available from: http://sukjaro.eu/myDAQ_Manual.pdf.
40. *STRAIN GAGE ACCESSORIES*. Available from: https://www.omega.com/pressure/pdf/ref_straingage_install.pdf.